



**Politecnico
di Torino**

Facoltà di ingegneria

Laurea Magistrale

in Ingegneria Aerospaziale

Evaluation of the Arbitrary Lagrangian-Eulerian method (ALE) for the simulation of Fluid-Structure interaction during aircraft ditching events

Candidato:

Corrado Amato

Relatore:

Prof. Giacomo Frulla

Corelatore:

Prof. Enrico Cestino

Supervisor esterni:

*Dieter Kohlgrüber
Christian Leon Munoz*

Tesi svolta all'estero in collaborazione tra
POLITECNICO DI TORINO e DLR



**Politecnico
di Torino**



Facoltà di ingegneria

Laurea Magistrale

in Ingegneria Aerospaziale

Evaluation of the Arbitrary Lagrangian-Eulerian method
(ALE) for the simulation of Fluid-Structure interaction
during aircraft ditching events

Candidato:

Corrado Amato

Relatore:

Prof. Giacomo Frulla

Corelatore:

Prof. Enrico Cestino

Supervisor esterni:

*Dieter Kohlgrüber
Christian Leon Munoz*

The dissemination of company data and information reported in this study has been approved by the DLR.

Acknowledgements

I would like to thank the whole team of Stuttgart at DLR for their warm welcome and for the help they gave me during my master thesis. In particular, I would like to thank Dieter Kohlgrüber and Christian Leon Munoz who accompanied and advised me during my stay at DLR.

I would also like to thank my Professors Giacomo Frulla and Enrico Cestino and Politecnico di Torino for providing me with the opportunity of such an experience at the German Aerospace Center.

Contents

1	Introduction.....	7
1.1	German Aerospace Center - DLR.....	7
1.2	Institute of Structure and Design	7
1.3	Stuttgart Integrity Department	8
1.4	Background and motivation of the work.....	8
2	Arbitrary Lagrangian Eulerian method in Fluid-Structure Interaction.....	10
2.1	ALE in LS-DYNA	11
3	Model generation process using PANDORA.....	13
4	Benchmarks	14
4.1	Sphere Free Fall.....	14
4.1.1	Problem description	14
4.1.2	Numerical model.....	14
4.1.3	Numerical results	16
4.1.4	Conclusion	17
4.2	Single Flat Panel	17
4.2.1	Panel in a guided motion.....	18
4.2.2	Water impact Numerical model	21
4.2.3	Numerical results	22
4.2.4	Conclusion	24
4.3	Double-Curved Panel.....	24
4.3.1	Numerical model.....	25
4.3.2	Influence of the refinement in the pressure distribution.....	27
4.3.3	Numerical results	28
4.3.4	Conclusion	30
4.4	D150 rigid aircraft.....	31
4.4.1	Numerical model.....	31
4.4.2	Numerical results	32
4.4.3	Conclusion	35
5	Conclusion and Outlook	36
5.1	Conclusion	36
5.2	Outlook.....	36
6	Bibliography.....	38

List of Figures

Figure 1: Establishment of DLR in Germany	7
Figure 2: Stuttgart offices	8
Figure 3: Ditching phases [1]	8
Figure 4: Lagrangian, Eulerian and ALE mesh and material motion [2]	10
Figure 5: Lagrangian and Intermediate steps of ALE [3]	11
Figure 6: Penalty coupling method [3].....	11
Figure 7: Refined pool generated automatically with PANDORA	13
Figure 8: Summary of models to analyze. The model with white background is not analyzed in this study	14
Figure 9: Sphere Free Fall on LS-DYNA: a) isoview; b) front view	15
Figure 10: Acceleration in z direction for SFF model	16
Figure 11: Guided ditching experimental facility [1]	18
Figure 12: a) Structural model Measures are in millimeters [1]; b) Rigid panel with strain gauges and pressure probes	18
Figure 13: Application of the two forces	19
Figure 14: Reaction forces Flat Panel free fly	20
Figure 15: Guided flat panel LS-DYNA model: a) water and vacuum mesh; b) water, structural model and vacuum.	21
Figure 16: Comparison of reaction forces between ALE model and experimental data [2]	22
Figure 17: Comparison of the pressure between ALE and experimental data [2]	23
Figure 18: Location of the DCP with respect to circular-elliptical cross section fuselage [3]	24
Figure 19: Representation of the DCP experimental facility and panel [4]	25
Figure 20: Probes distribution on the panel [4]	25
Figure 21: Structural model [13].....	26
Figure 22: Guided Double-Curved Panel LS-DYNA model: a) water and air mesh; b) water, structural model and air	26
Figure 23: Comparison of the pressure distribution between models without (left) and with refinement (right)	27
Figure 24: Comparison of the reaction force between ALE model and experimental data	28
Figure 25: Pressure for the front probes of the DCP	29
Figure 26: Comparison of the pressure between ALE model and experimental data [13] for the rear probes of the DCP	29
Figure 27: DCP simulation at 20 ms, 40 ms, 55 ms and 66 ms from top left to the right bottom	30
Figure 28: Dimension D150 Aircraft [6]	31
Figure 29: D150 model on LS-DYNA: a) water and air mesh; b) water, structural model and air.	31
Figure 30: Pitch angle D150	33
Figure 31: Contact force D150	33
Figure 32: Displacement along Z direction of the D150 COG	33
Figure 33: D150 simulation (iso and left side view) and pressure (top view) at 150 ms, 250 ms, 350 ms and 450 ms from top to the bottom.....	34

List of Tables

Table 1: EOS parameters	15
Table 2: Computational results for 3 EOS.....	17
Table 3: Flat panel free fly model parameters.....	19
Table 4: Reaction forces in global.....	20
Table 5: Water and vacuum setting.....	22
Table 6: Refinement setting.....	22
Table 7: Comparison of the first peak for each probe between ALE and experimental data.....	23
Table 8: Computational results for rigid flat panel.....	24
Table 9: Water and air basins setting	27
Table 10: Computational results for the Double-Curved Panel.....	30
Table 11: Moments of inertia of D150. All the parameters are in kg·mm ²	32
Table 12: Water and air basins setting	32
Table 13: Refinement setting.....	32
Table 14: Computational results for D150.....	35

Glossary and definitions

ALE:	Arbitrary Lagrangian Eulerian
SPH:	Smoothed Particle Hydrodynamics
FE:	Finite Element
FSI:	Fluid-Structure Interaction
ONERA:	Office National d'Études et de Recherches Aérospatiales
SFF:	Sphere Free Fall
EOS:	Equation Of State
SMAES:	Smart Aircraft in Emergency Situations
SARAH:	Increased Safety and Robust certification for ditching of Aircraft and Helicopters
RADIAN:	Robust Aircraft Ditching Analysis
ADAWI:	Assessment of Aircraft Ditching and Water Impact
GDS:	Guided Ditching Simulation
PANDORA:	Parametric Numerical Design and Optimization Routines for Aircraft
CPACS:	Common Parametric Aircraft Configuration Schema
LS-DYNA:	Advanced general-purpose Multiphysics simulation software package by LSTC

1 Introduction

1.1 German Aerospace Center - DLR

The German Aerospace centre (Deutsches Zentrum für Luft und Raumfahrt – DLR) is the national aeronautics and space research centre of Germany. Its headquarters are located in Cologne, it has multiple other location throughout Germany. DLR’s work is diverse and geared towards the needs of society. It focused on research in the areas of mobility, energy, communications, security, digitalisation, aeronautics and space. DLR uses the expertise of its 55 research institutes and facilities to develop solutions in these areas. The 10.000 employees share a mission to explore Earth and space and develop technologies for a sustainable future. In doing so, DLR contributes to strengthening Germany’s position as a prime location for research and industry.



Figure 1: Establishment of DLR in Germany

1.2 Institute of Structure and Design

The institute of Structure and Design is based on two locations: Stuttgart (Fig. 2) and Augsburg. The institute of Stuttgart is composed of five departments working on the development of high-performance solutions in the fields of aeronautics, aerospace, transportation, energy and mechanical engineering. The scientific work in Stuttgart ranges from the development and optimisation of materials and their process and joining technologies to new design approaches, the construction of full-scale demonstrators and their testing and validation in specific test facilities and in-flight tests. The focus is on fibre reinforced ceramic, polymeric and hybrid composites. The development of new multidisciplinary design tools and digital models is the basis for the development of new technologies.



Figure 2: Stuttgart offices

1.3 Stuttgart Integrity Department

The Structural Integrity department works on the development and numerical simulations of multifunctional lightweight structures made of metallic, composite or hybrid materials. This includes material and structure tests as well as numerical analyses from sample level up to full-scale structures. The research work focuses on the transient dynamic load cases like crash, ditching and high-velocity impact of various impactors like birds, hail, tire pieces, drones, etc. The main objective of new design developments is the improvement of energy absorption capacity and thus operation safety without noticeably impairing the loadbearing capacity and increasing weight. Furthermore, the department develops numerical process chains for automatic modelling and simulation of structures for integration into multidisciplinary analysis and optimization chains.

1.4 Background and motivation of the work

One of the possible scenarios for an aircraft is the ditching: an emergency landing on the water. Over the years the percentage of ditching compared to the number of flights performed has decreased, thanks to the greater safety in airplanes compared to the past. Even if nowadays a ditching is less likely, it is still possible.

As it is shown in the Fig. 3 there are 4 phases of the ditching: approach, impact, landing and floatation.



Figure 3: Ditching phases [1]

In the first phase, approach, to maintain a low speed and the nose up of the aircraft is important. There are also some recommended configurations of the aircraft components to lower the impact velocity.

Then, the second phase, impact, starts when the bottom rear part of the fuselage comes into contact with the water. This is the highest load phase for the aircraft. The third phase is the landing between touchdown and stillstand of the aircraft, this is the phase where hydrodynamic phenomena occur. In the last phase, the aircraft is evacuated.

To Simulate ditching, and in particular the impact, there are different numerical methods, one of these is the Arbitrary Lagrangian-Eulerian (ALE) method, it is applied through the software LS-DYNA. Thanks to simulations it is possible to predict forces applied to the structure, the consequences of that and it is also important to estimate the available evacuation time for passengers and crew during the floatation.

The Institute of Structures and Design (BT) of the German Aerospace Center (DLR) has a long research background in the field of the planned emergency landing on water. The investigation of the behaviour of an aircraft during ditching is mandatory in the certification process according to crashworthiness certification requirements. The research at DLR-BT concentrates on the impact and the landing phases of fixed-wing aircraft.

According to the precedent studies at DLR-BT for ditching analysis, the first method used was the coupled SPH-FE where the main fluid domain discretized using SPH particles is surrounded by Volume Elements (FE). Using this approach, method comparison was conducted with similar ALE models from ONERA like in the common research project RADIANT. The ALE method was then assessed at DLR in the scope of the project PRESTO-LX [6] for water impact problems, where first computations were launched and a first global understanding of the method using LS-DYNA could be achieved. However, not all benchmarks intended to be assessed in the project could be analysed with ALE and a more detailed investigation of the method in LS-DYNA is still missing.

The objective is the assessment of the ALE method for ditching simulations. In the next chapters, after an explanation of the ALE method and an internal software at DLR, called PANDORA, four models have been analysed in LS-DYNA: the Sphere Free Fall (SFF), the guided rigid flat panel [1][2], the guided double curved panel [3][4] and the D150 aircraft.

2 Arbitrary Lagrangian Eulerian method in Fluid-Structure Interaction

The Arbitrary Lagrangian-Eulerian method contains two algorithms, Lagrangian and Eulerian, what ALE does is to combine the advantages of them minimizing their respective drawbacks.

The Lagrangian algorithm is based on the movement of the nodes of the computational mesh that follow the associated material. This is not a good method for large deformations.

In the Eulerian method the computational mesh is fixed, the material moves independently from it. This method can easily handle large deformations.

In the ALE the nodes of the computational methods can be moved in some arbitrary way and the material can flow through the mesh as we can see in the Fig. 4.

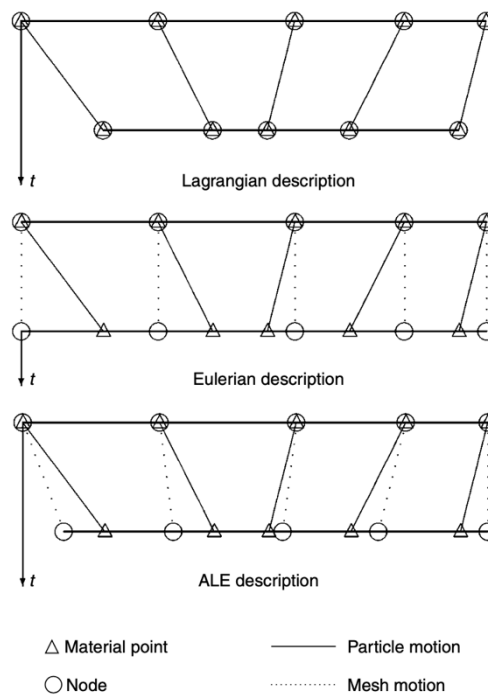


Figure 4: Lagrangian, Eulerian and ALE mesh and material motion [2]

Thanks to this arbitrary movement of the mesh, ALE method can manage large distortions with a better resolution compared to the Eulerian algorithm. It permits to the ALE method to be applied in different engineering fields, like manufacturing, fluid-structure interaction and coupling of multi-physics fields with multi-materials.

In each ALE time iteration, there are 2 steps: lagrangian and intermediate. The first one consists in a lagrangian structure completely immersed in an eulerian mesh, it consists in the movement of the structure and, as consequence, the distortion of the nodes tied to the structure.

In the intermediate step there are 2 phases (see Fig. 5), the first one is the mesh smoothing in which the distorted nodes come to the original position, to do it there are different algorithms available: equipotential smoothing, simple averaging smoothing, surface smoothing and others. The second phase of the intermediate step is called advection in which, since the mesh smoothing, the structure flows from an element of the mesh to a different one and the variables must be recalculated.

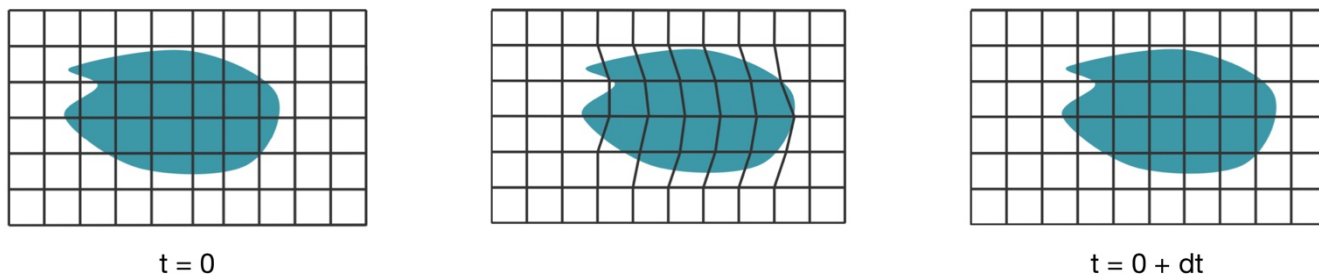


Figure 5: Lagrangian and Intermediate steps of ALE [3]

2.1 ALE in LS-DYNA

An advection algorithm is good if it is accurate, stable, conservative and monotonic, in LS-DYNA two algorithms are available for the advection step: Donor Cell and Van Leer. Although the former is a first order accuracy algorithm it is stable and monotonic, instead, the latter is a second order accuracy: it means that now, the variable is regarded as the average value over the whole element instead of the spatial value only at the center of the element. Both algorithms are used with Half Index Shift (HIS) algorithm, able to overcome dispersion errors and to preserve the monotonicity of the velocity field [7]. All the models showed in this report have been made with Van Leer advection algorithm, set in the ***Control_ALE** card for a better accuracy.

The ALE method uses the penalty coupling formulation. This algorithm calculates the relative displacement between fluid and structure, then nodal forces are developed and applied to the lagrangian and eulerian materials in the opposite direction (see Fig. 6)

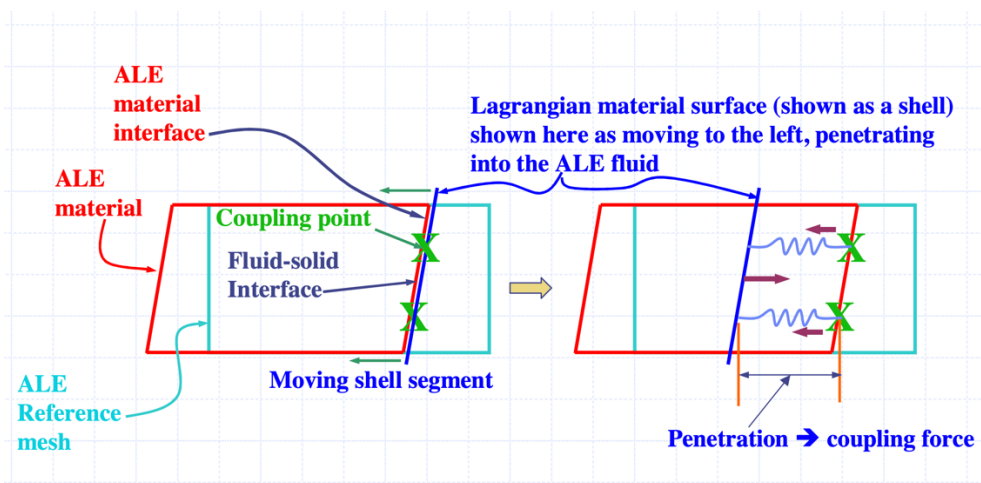


Figure 6: Penalty coupling method [3]

The nodal forces generated depends on distance d between fluid and structure and on stiffness factor k .

$$f = d \cdot k$$

The distance d is updated each cycle, stiffness factor follows this formula:

$$k = f_s \frac{K_i \cdot A_i^2}{V_i}$$

The first parameter f_s is the scale factor for the interface stiffness, its value is between 0 and 1 but the default value is 0.1; K_i is the bulk modulus, V_i is the volume of the element that contains master nodes (eulerian material) and A_i is the face area of the elements that contains the master segment.

3 Model generation process using PANDORA

Models analyzed with LS-DYNA are created in PANDORA (Parametric Numerical Design and Optimization Routines for Aircraft), a software framework for the aircraft structural analysis developed by DLR based on Python language [9]. Operations in PANDORA can be performed by independent packages dedicated for specific functions: CPACS (Common Parametric Aircraft Configuration Schema) based, FE-data based and other utility packages. One of the FE-data packages is called FE_CONVERTER, it allows to provide conversion from and to specific solver files. A Graphical User Interface (GUI) has been implemented to allow users without previous experience with python source code to use PANDORA [9]. Once a file `.h5` containing the structure is imported in PANDORA GUI, it's possible to check all the data of the model in the FAW RAW command: nodes, elements, properties, materials, local coordinates systems, boundary conditions and general settings related to the simulation.

One of the new packages available in PANDORA, called FE_DITCHING, allows to generate the fluid model and include FSI features. Fluid-Structure Interaction (FSI) represents the interaction between a fluid flow and a structure, the consequences of that are pressure and loads exerted on the structure. With the implemented Python routines, it is possible to generate the fluid model for different numerical fluid modelling approaches. In general, it's possible to define the size of the pool according to the model, then, focusing on ALE method, the basins of water and vacuum are created [10]. The implemented features specifically for ALE method are:

- 1) the resolution of the general mesh or of the refinement if it is switched on;
- 2) to change the direction of the shells normal vector that, for a correct coupling between lagrangian structure and eulerian elements, must face the fluid in according to the ALE method;
- 3) to define a different height of the vacuum basin;
- 4) to set a different mesh size in z direction;
- 5) to save computational time it's also possible to set the dimensions of a refinement zone.

The refinement is a part of the entire pool with a finer mesh, outside this area the size of the element starts to increase up to a limit value which can be set in advance.

After all the parameters just described have been set, the pool can be generated (see Fig. 7). The boundary conditions, such as nodal constraints (SPC), are automatically generated in all the outermost nodes of the pool. Now the model is ready to be exported in LS-DYNA thanks to the package FE_CONVERTED mentioned above.

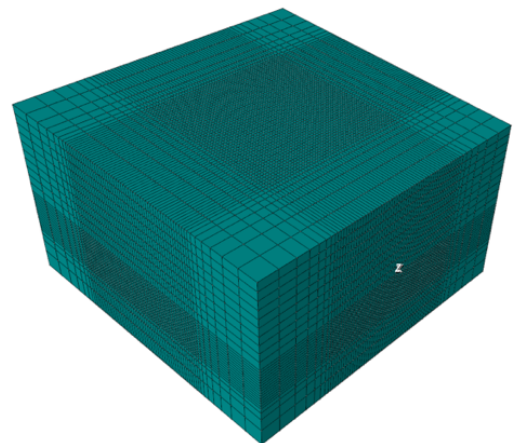


Figure 7: Refined pool generated automatically with PANDORA

4 Benchmarks

The models to be analyzed start from simple structures to an entire rigid aircraft. The first model, analyzed in the next paragraph, is a rigid sphere into water with a vertical initial velocity, followed by 2 rigid guided panels: the first is a Flat Panel (FP) that belongs to SMAES project [11], then there is a Double-Curved Panel (DCP) from SARAH project [12]. At the end, a rigid aircraft including the parameters of previous benchmarks is analyzed to simulate the global kinematics during a ditch (see Fig. 8).

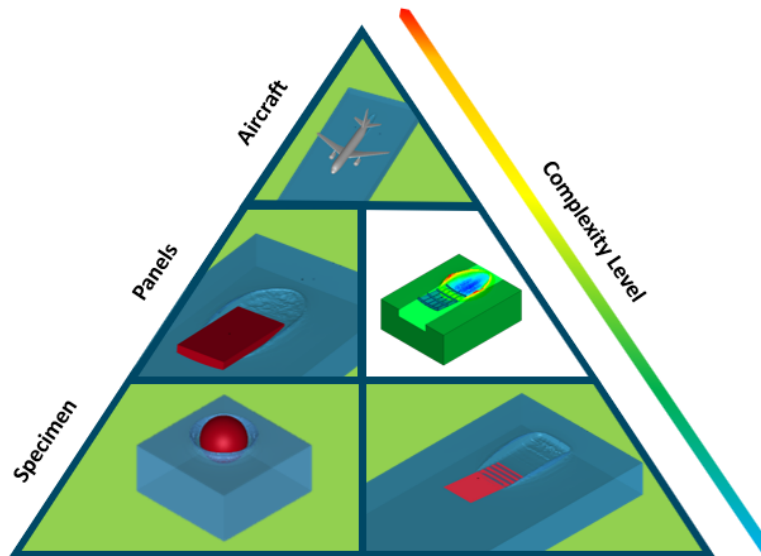


Figure 8: Summary of models to analyze. The model with white background is not analyzed in this study

4.1 Sphere Free Fall

4.1.1 Problem description

This model represents the vertical drop of a rigid sphere into water, it has been already analyzed at DLR [13], the study here focuses more on the use of different Equation Of States (EOS). Results obtained with ALE method will be compared to experimental data by Marco Anghileri [14].

4.1.2 Numerical model

The model contains a sphere with a radius of 109 mm. The rigid metallic sphere is defined with 3750 quad shell elements with a predefined mass of 3.76 kg, it has a density of 2800 kg/m^3 . Regarding the fluid, in the model there are 2 different kinds of domains: one is water defined with a density of 1000

kg/m³; the other is modelled as vacuum, defining its density equal to 1·10⁻³ kg/m³. Each basin has 627200 solid elements.

All outermost nodes of the domains are fixed with the card *BOUNDARY_SPC_SET, all 6 degrees of freedom are constrained.

The length and width for each basin are 560 mm, the height of the water basin and of the vacuum basin is respectively of 250 mm (see Fig. 9).

The mesh size of each element for both domains is 5 mm and the simulation time is 20 ms.

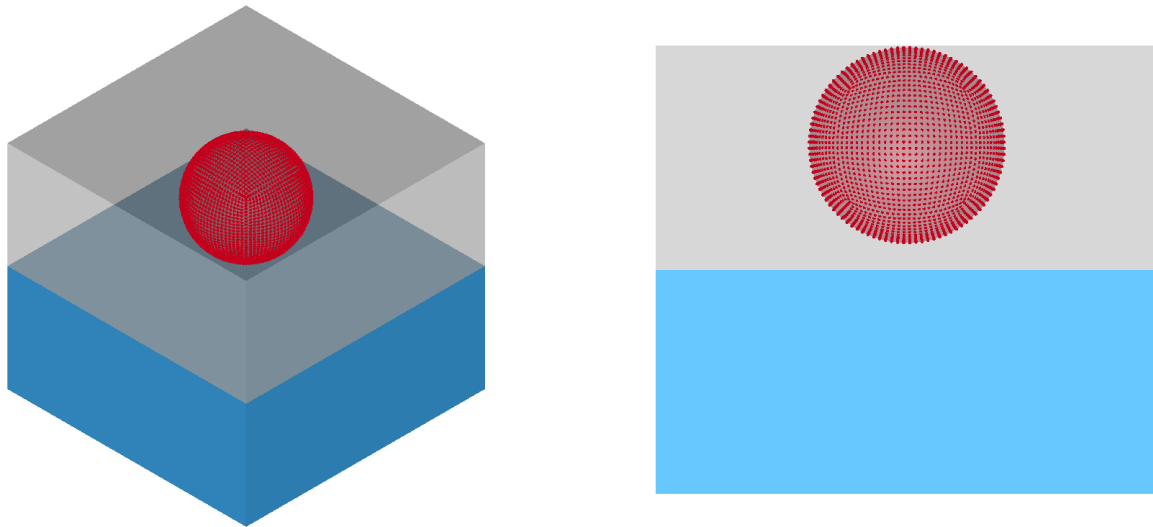


Figure 9: Sphere Free Fall on LS-DYNA: a) isoview; b) front view

An initial velocity of 11.8 m/s is applied to the sphere and a gravity of 9.81 m/s² is applied to the entire model. Moreover, the number of coupling points distributed over each coupled lagrangian surface segment has been set equal to 4 in order to obtain a high accuracy during coupling.

A study about different Equations Of State (EOS) was conducted: Linear polynomial, Gruneisen and Murnaghan.

In the Table 1 the details for each EOS are shown.

EOS	Parameters		
Gruneisen [8]	$C = 1483 \text{ m/s}$	$S1 = 1.75$	$\gamma_0 = 0.28$
Linear polynomial [9]	$C_1 = 2.72 \text{ GPa}$	$C_2 = 7.727 \text{ GPa}$	$C_3 = 14.66 \text{ GPa}$
Murnaghan [9]	$\gamma = 7$	$k_0 = 0.144 \text{ GPa}$	

Table 1: EOS parameters

Below are the formulas regarding pressure for each EOS.

- Gruneisen:

$$p = \frac{\rho_0 C^2 \mu \left[1 + \left(1 - \frac{\gamma_0}{2} \right) \mu - \frac{a}{2} \mu^2 \right]} \left[1 - (S_1 - 1) \mu - S_2 \frac{\mu^2}{\mu + 1} - S_3 \frac{\mu^3}{(\mu + 1)^2} \right]^2 + (\gamma_0 + a \mu) E$$

- Linear polynomial:

$$p = C_0 + C_1 \mu + C_2 \mu^2 + C_3 \mu^3 + (C_4 + C_5 \mu + C_6 \mu^2) E$$

- Murnaghan:

$$p = k_0 \left[\left(\frac{\rho}{\rho_0} \right)^\gamma - 1 \right]$$

If some parameters are not in the Table 1 means their values are equal to zero in the formulas, for more information see [17].

4.1.3 Numerical results

In the Fig. 10 the black curve comes from experimental data by Marco Anghileri [14].

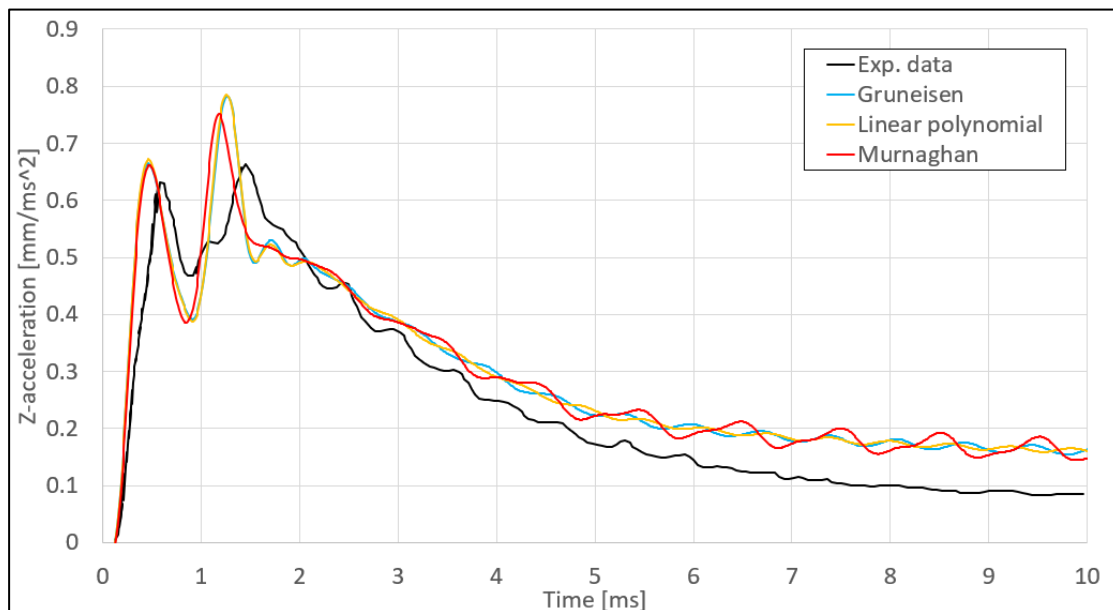


Figure 10: Acceleration in z direction for SFF model

The behavior of the curves is similar independently of the EOS, the main points out are:

- The first peak is very good simulated with ALE. About the experimental curve the peak reaches the value of 0.63 mm/ms^2 , ALE curves reach the value of 0.66 mm/ms^2 , it corresponds to 4.5% more;
- Regarding the second peak, the Linear Polynomial and Gruneisen EOS have an higher value (0.78 mm/ms^2) than Murnaghan curve (0.74 mm/ms^2), it means respectively a difference of 20% and almost 14% compared to the experimental curve peak (0.65 mm/s^2);
- Starting from 3 ms, the Murnaghan curve has bigger oscillations compared to the other 2 EOS;
- Starting around 2.5 ms the distance between ALE curves and experimental data increases more and more up to the end of the simulation when the difference is equal to 0.08 mm/ms^2 .

For all the simulations have been used 4 computational nodes and a total of 32 cores, the smallest timestep is $6.99\text{E-}04 \text{ ms}$ and the number of iterations is 28615. The Table 2 shows the elapsed time for each EOS.

	Elapsed time
Gruneisen	3h 04' 15''
Linear polynomial	2h 30' 13''
Murnaghan	3h 00' 38'

Table 2: Computational results for 3 EOS

4.1.4 Conclusion

The acceleration curve in z direction with ALE method is similar to the experimental curve for all 3 EOS that, apart from the bigger oscillations of the Murnaghan curve, have the same trend. To understand which EOS to choose to continue with next models, computational parameters must be analyzed. From the elapsed time Linear Polynomial is the fastest EOS, so for all next benchmarks this EOS is set.

4.2 Single Flat Panel

A guided single flat panel is the second model to analyze. The entire structure contains a guide track, a trolley that holds the panel and a catapult-type acceleration system.

The Fig. 11 shows experimental facility used for the research project SMAES. The five height-adjustable bridges allow the variation of the guide track inclination, the catapult-like acceleration system consist of elastic cods to accelerate the main trolley holding the test specimens and an auxiliary trolley holding

the elastic cords. The deceleration occurs thanks to a braking system activated after the relevant impact phase.

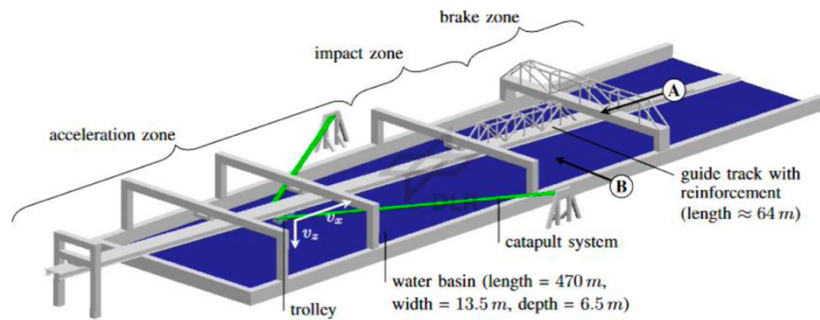


Figure 11: Guided ditching experimental facility [1]

In the SMAES project different kind of flat panels have been studied, among which a quasi-rigid specimen. The panel is riveted to an L-shaped frame. On the panel there are accelerometers, strain gauges and pressure probes (see Fig. 12).

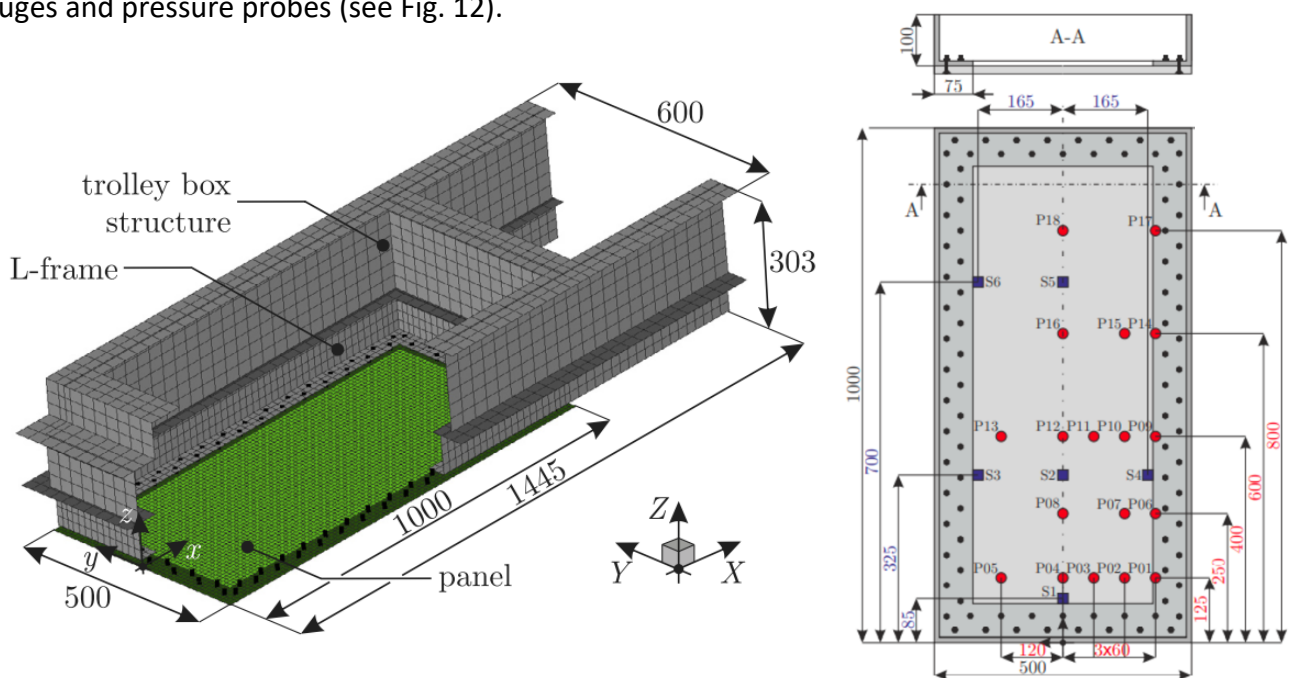


Figure 12: a) Structural model Measures are in millimeters [1]; b) Rigid panel with strain gauges and pressure

4.2.1 Panel in a guided motion

Before to move to a complete model with ALE element, it was decided to start a study with the flat panel in a free flight motion, to understand the convenient setup how to extract reaction forces from LS-DYNA.

The first attempts to set gravity and constraints in the movement of the panel contained following keywords:

- ***Boundary_prescribed_motion_set** to include gravity in the model.
- ***Boundary_spc_node** to allow to the panel to move only in specific directions.

Using these keywords, the displacement in z direction obtained was incorrect compared to the expected displacement according to the predefined motion. For this reason, in the next models the keywords above were replaced by:

- ***Load_body_z** to include gravity in z direction.
- ***Constrained_nodal_rigid_body_spc_inertia** to add constraints to the panel.

Thanks to these two last keywords, the displacement is now the one expected.

To extract forces from a rigid body in LS-DYNA, the study started with analytical calculations of reaction forces in a model without gravity.

In the model the force is applied in two different points in Z global direction on the rear part of the model as it is possible to see in the Fig. 13. Each force applied is equal to 100 kN. The forces are no activated at the begin of the simulation, but they start to act at 20 ms.

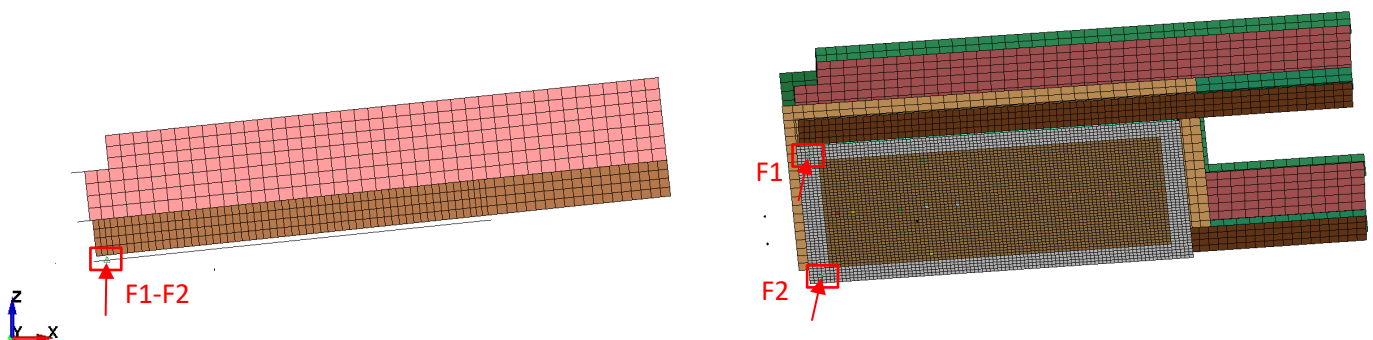


Figure 13: Application of the two forces

In the Table 3 there are the features of the model.

Simulation time	Local Velocity x	Track inclination α	Mass rigid body	Total force
100 ms	46 mm/ms	30°	838.119 kg	200 kN

Table 3: Flat panel free fly model parameters

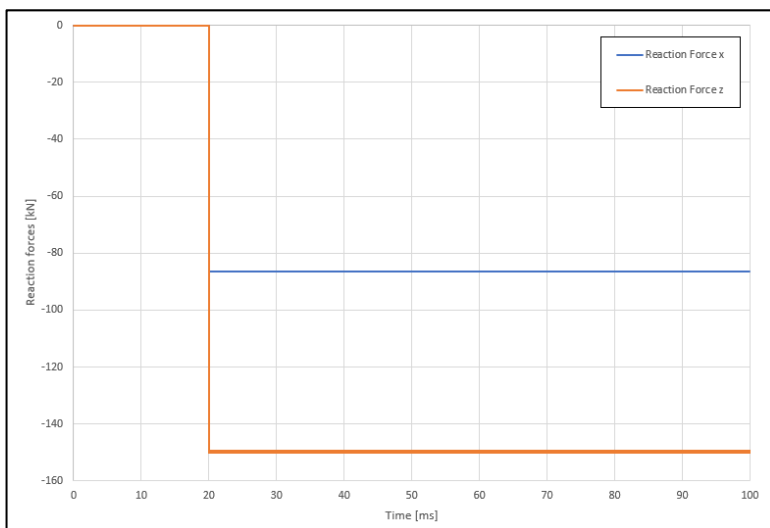
After a check of velocities and displacements respectively in the file *nodout* and *g/stat*, generated by LS-DYNA during the simulation, it's possible to check if reaction forces from LS-DYNA are same of analytical forces.

The expected forces in local coordinate are:

- $F_{z,loc} = \cos(\alpha) \cdot 200 \text{ kN} = 173.205 \text{ kN}$
- $F_{x,loc} = \sin(\alpha) \cdot 200 \text{ kN} = 100 \text{ kN}$

To plot reaction forces from a rigid body in LS-DYNA the parameter *SPC2BND*, in the keyword ***Control_output**, must be set to 1 from 0 (default value), and the option *bndout* must be activated in the keyword ***Database_option**. Then a file called *bndout* will be generated in the same folder of the .k file.

From the model in LS-DYNA is not possible to obtain reaction forces in local coordinates so far, the forces in the next graph are in global coordinate.



React. Force x	React. Force z
-86.415 kN	-150.217 kN

Table 4: Reaction forces in global coordinate system

Figure 14: Reaction forces Flat Panel free fly

Moving the values of reaction forces of the Fig. 14 in z local direction, as it is shown in the next formula, the resultant force $R_{z,loc}$ is -173.29 kN, really close to the theoretical value of 173.205 kN.

$$R_{z,loc} = R_{z,glo} \cdot \cos(\alpha) + R_{x,glo} \cdot \sin(\alpha) = -173.29 \text{ kN}$$

The negative sign of the reaction forces is justified by the application of the total force in positive z direction.

Regarding reaction force in x local direction, it's possible to calculate it by means of acceleration in local coordinates.

$$R_{x,loc} = a_{x,loc} \cdot m = -0.118991 \cdot 838.119 = -99.73 \text{ kN}$$

The acceleration $a_{x,loc}$ is in the file *nodout* at the end of the simulation, the total mass of the rigid body m is predefined.

The value obtained is again very close to the theoretical one equal to 100 kN.

This flat panel free fly model is without gravity, including it then, in order to extract only the reaction force in z direction, the gravity must be compensated subtracting the relative force.

$$F_{z,gra} = m \cdot g \cdot \cos(\alpha) = 838.119 \cdot 0.00981 \cdot \cos(30^\circ) = 7.12 \text{ kN}$$

This compensation must be done in x local coordinates too, the final value of the reaction force in x local coordinates, extracting by means of acceleration, is obtained in the following way.

$$F_{x,loc} = m \cdot a_{x,loc} - m \cdot g \cdot \sin(\alpha) = m \cdot [a_{x,loc} - g \cdot \sin(\alpha)]$$

In this way it's possible to obtain reaction forces in local coordinates from a rigid guided body in models that include gravity.

Force can be extracted also from contact force, it is obtained from the output file *dbfsi*, generated when the card ***Database_fsi** is set. It represents the force of the fluid-structure interaction.

4.2.2 Water impact Numerical model

The numerical structural model includes trolley box structure, L-frame and panel. Simulation time is 80 ms including the impact and landing. The panel has a sink rate in z direction of 1.5 m/s and a forward velocity of 40 m/s in global coordinates, moreover there is a pitch angle of 6°. In LS-DYNA only one velocity of 40.028 m/s has been implemented with the keyword ***Initial_velocity** because it allows to enter velocities in local coordinates by means of parameter **ICID**. The local coordinate system has the path of the panel as x axis. As it is shown in the table 5, this model has a refinement zone in the impact zone (see Fig. 15). The mass of the rigid body is 838.119 kg.

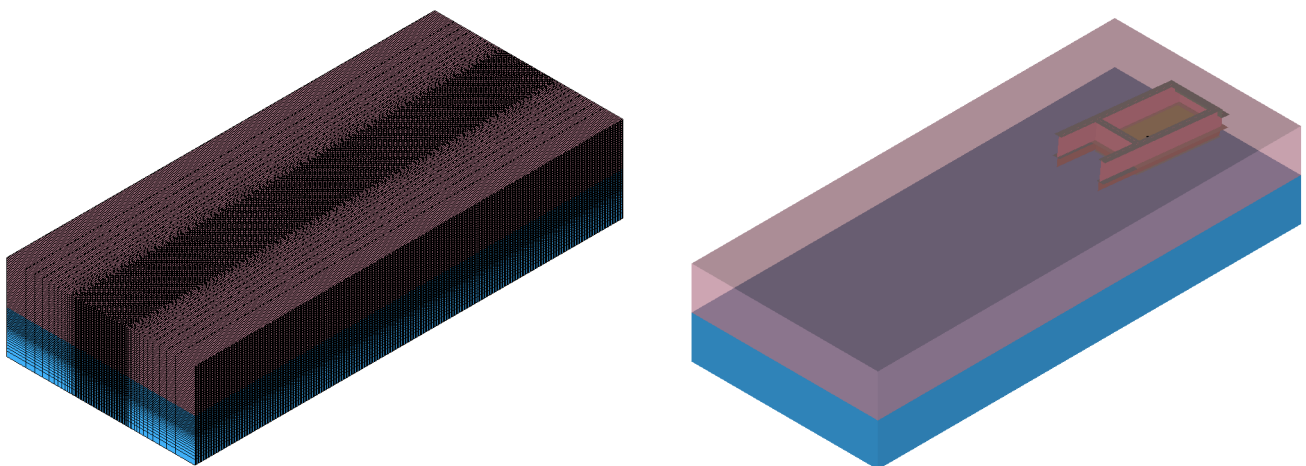


Figure 15: Guided flat panel LS-DYNA model: a) water and vacuum mesh; b) water, structural model and vacuum.

In the Tables 5 and 6 general parameters about the two domains water and vacuum are shown.

Size each domain (length x, width y, height z)	N. elements of water	N. elements of vacuum
(5000, 2200, 500) mm	1 452 000	2 200 000

Table 5: Water and vacuum setting

Mesh water refinement size	Length x direction	Width y direction	Height z direction
10 mm	5000 mm	600 mm	200 mm

Table 6: Refinement setting

To extract pressure there are probes, the main probes selected to analyze pressure are P04, P08, P12, P16 and P18, located in the center along the entire panel (see figure 10). In LS_DYNA, to extract pressure by these sensors it's possible set the keyword ***Database_fsi_sensor**.

4.2.3 Numerical results

Starting from a global point of view analyzing the reaction force, the Fig. 16 shows the ALE curve approximates very well the experimental curve. Since on LS-DYNA is not possible to extract reaction forces in local coordinate system, to have a proper comparison with experimental data, the results in global coordinate system have been transformed in local

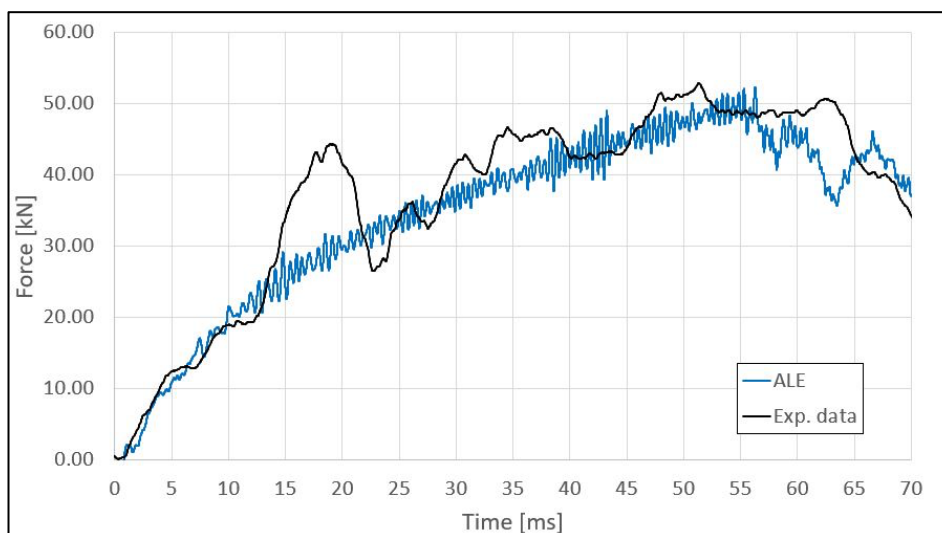


Figure 16: Comparison of reaction forces between ALE model and experimental data [2]

coordinated system. Moreover, the compensation of the gravity is needed, as it is explained in the paragraph 4.2.1. ALE curve doesn't highlight the peak of the experimental curve at 18 ms, in this case the black curve reaches the value of 44.8 kN, around 15 kN more than the blue curve. Starting from 28

ms to 40 ms, the ALE force is underestimated on average by 6 kN. In the final part of the simulation, from 55 ms, the ALE curve follows the decreasing trend of the experimental data. For the last 5 ms the ALE results overestimate the experimental curve of around 3kN.

Focusing now on the pressure, the Fig. 17 shows the comparison of 5 probes. To obtain a proper shape of the ALE pressure curves the size of the water and vacuum basins must be the same at the interface. The table 7 shows the difference for the peak values between ALE and experimental data.

The Table 7 shows that the highest difference is for the probe 18 with 0.69 MPa and on average there is a difference of 0.592 MPa.

Another point to highlight is the shape of the ALE curves, the decrease is not linear as experimental data but there is the return of each curve to zero along the entire simulation.

	Exp. Data [MPa]	ALE [MPa]	Difference [MPa - %]
P04	1.44	0.91	0.53 – 36.8%
P08	1.18	0.67	0.51 – 43.2%
P12	1.34	0.68	0.66 – 49.3%
P16	1.42	0.85	0.57 – 40.1%
P18	1.25	0.56	0.69 – 55.2%

Table 7: Comparison of the first peak for each probe between ALE and experimental data

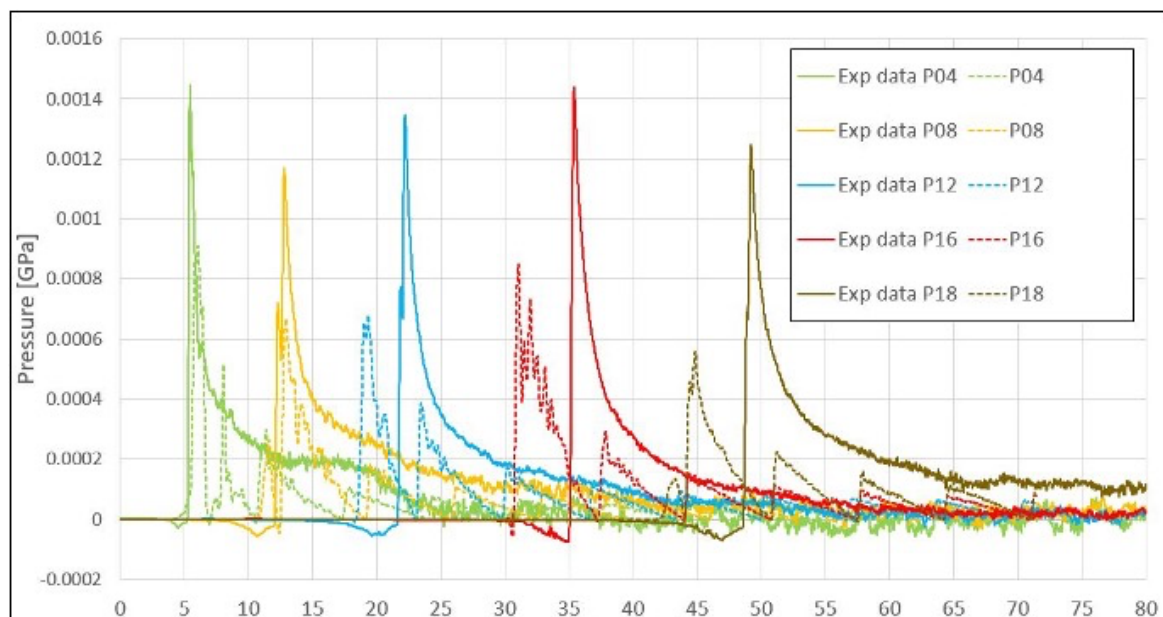


Figure 17: Comparison of the pressure between ALE and experimental data [2]

In the Table 8 some computational outputs are shown.

Elapsed time	Iterations	Smallest TS	Nodes	Cores	Solver version
10h 42' 22''	47 007	1.7019E-03 ms	1	16	R13.1

Table 8: Computational results for rigid flat panel

4.2.4 Conclusion

In the first part of the paragraph a study was conducted on how to extract reaction forces from a rigid body on LS-DYNA, analyzing the flat panel with a guided motion without water in both cases with and without gravity. Then water was included in the model comparing results with experimental data. From a global point of view the force is calculated well in the ALE model, with small differences from the experimental data. Regarding the local point of view, the pressure is underestimated for all 5 probes in the ALE method.

It is now possible to plot pressure by sensors with ALE model in LS-DYNA with the output card ***Database_fsi_sensor**, even if that card needs to be analyzed more because using solid elements, instead that shell elements, results more like the experimental data could be obtained.

Before to reach that results, different setups of this model have been analyzed and it is possible to confirm that to reach comparable results by pressure sensors the ALE elements at the interface must have the same size.

4.3 Double-Curved Panel

Next benchmark to analyze is the Double-Curved Panel, it is part of the SARA project with the purpose to study in more detail the hydrodynamic phenomena. The DCP is interesting because it is the first part impacting water during ditching events, it represents the rear fuselage part (Fig. 18).

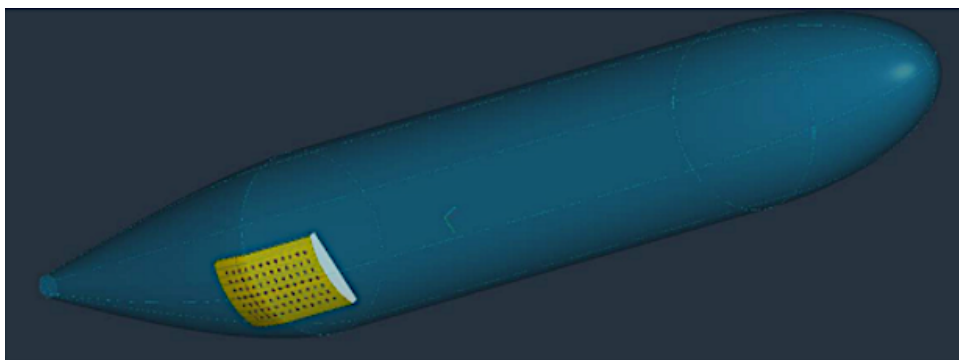


Figure 18: Location of the DCP with respect to circular-elliptical cross section fuselage [3]

The hydrodynamic phenomena expected from this model are cavitation and/or ventilation when the horizontal velocity exceeds a threshold limit.

- **Cavitation:** it represents the phase change of a fluid from liquid to vapor state due to the local pressure drop below the fluid's corresponding vapor pressure [1]. Cavitation

is related to the local increase of flow velocity and therefore to the drop of pressure, according to Bernoulli Principle.

- **Ventilation:** it occurs when trapped vapor reaches the end of the panel, higher pressure in the air led the cavity to ventilate and the pressure raised to the ambient pressure as the ventilation propagates forward.

The experimental facility (see Fig. 19) is the same used for the flat panel.

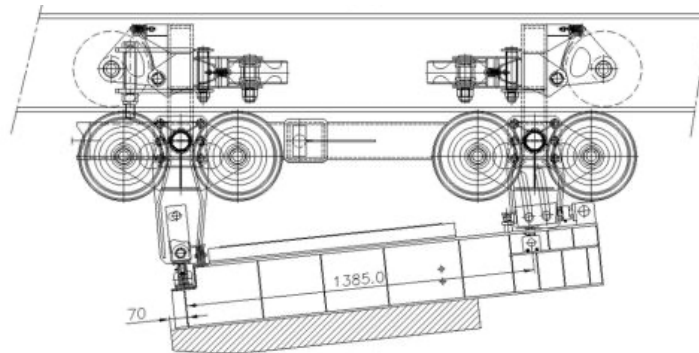


Figure 19: Representation of the DCP experimental facility and panel [4]

On the specimen, 30 probes have been installed with a more focus in the rear part of the panel as it is shown in the Fig. 20.

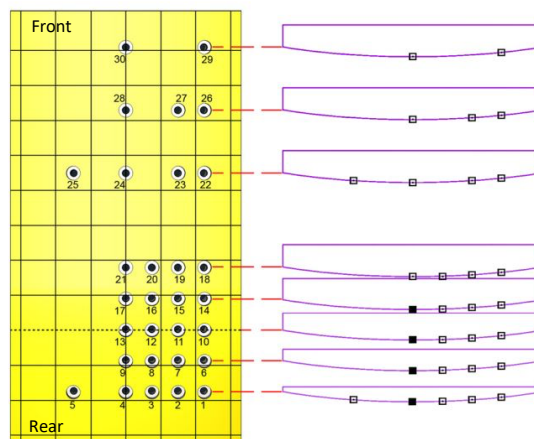


Figure 20: Probes distribution on the panel [4]

4.3.1 Numerical model

The structural model includes trolley box structure, L-frame and panel (Fig.21). Simulation time is 70 ms, the panel has a pitch angle of 6° , a sink rate in z direction of 1.5 m/s and a forward velocity of 40 m/s in global coordinates, but as for the flat panel, only one velocity of 40.028 m/s has been entered in local.

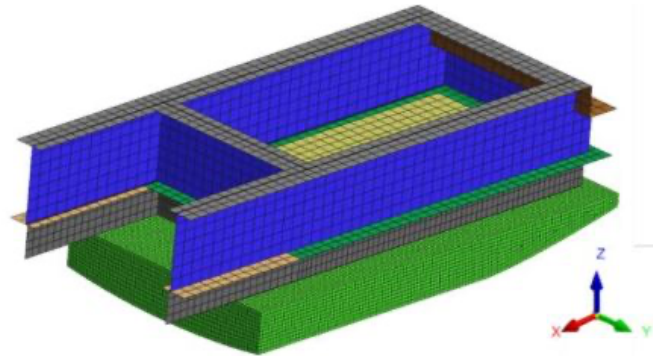


Figure 21: Structural model [13]

Unlike the flat panel in paragraph 4.2, for this benchmark all the solid elements of the water and upper basin have the same mesh size of 10 mm (Fig. 22) because a possible refinement could affect the results related to pressure by decreasing their accuracy (as it is described in the next paragraph). In this benchmark the focus is mainly on hydrodynamic phenomena and therefore a higher accuracy is intended. Furthermore, for this model air replaces vacuum because to simulate cavitation the fluid parameters must be as realistic as possible. Vacuum is defined with the ***Mat_vacuum** in which it's possible to define only density, instead air is defined by ***Mat_null** card setting, apart from density that for air is equal to 1 kg/m^3 , the viscosity equal to $1.8 \cdot 10^{-5} \text{ kg/(m} \cdot \text{s)}$. Air also requires EOS, linear polynomial has been set entering only $C0 = 101325 \text{ Pa}$, taking as reference the ambient pressure. Even for water $C0$ is equal to 101325 Pa for this model, unlike the two previous models where its value was equal to 0.

In addition, a second difference compared to the Flat Panel is the parameter DIREC in the ***Constrained_lagrange_in_solid** card. This parameter defined the coupling direction, for the previous benchmarks $\text{DIREC} = 2$ has been used, defining the coupling under normal direction, in compression only. For the DCP the value of DIREC is equal to 1 defining again the coupling under normal direction but in both tension and compression in this case [18].

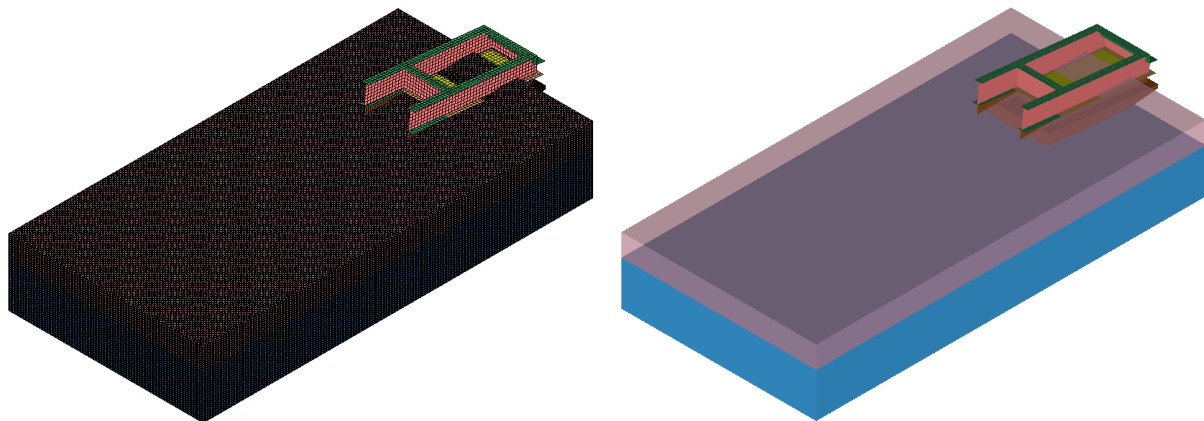


Figure 22: Guided Double-Curved Panel LS-DYNA model: a) water and air mesh; b) water, structural model and air.

In combination with the parameter DIREC, also the parameter EBC in the ***Control_ale** card has been changed from 0 (off) to 1 (stick condition) compared to the previous benchmarks. It defines the automatic Eulerian boundary condition [18]. Varying EBC from 0 to 2 (slip condition), setting DIREC = 1, it has no influence on the results. However, in according to [13], EBC = 0 or EBC = 2, could lead to instabilities. For this reason, EBC = 1 has been set up for the DCP.

Based on the previous benchmark, the number of solid elements for void is over 50% more than solid elements representing water, it is not efficient. To improve the model efficiency and to reduce computational time, some tests has been performed to understand the influence of the initial contact between SPCs, in the border nodes, and the lagrangian structure. The results didn't show any instability or other problem: it's possible to reduce the height of the upper basin even below the upper limit of the lagrangian structure.

In the Table 9 general parameters about the two domains water and air are shown.

Size water domain (length x, width y, height z)	Size air domain (length x, width y, height z)	N. elements of water	N. elements of air
(4400, 2200, 500) mm	(4400, 2200, 250) mm	4 840 000	2 420 000

Table 9: Water and air basins setting

4.3.2 Influence of the refinement in the pressure distribution

As it is written in the chapter 3, it's possible to generate the model with a refinement zone in the water basin. However, after a study, it's clear that the inhomogeneity of the mesh of the water basin has an influence on the pressure distribution in z direction. It could affect the results of the pressure in case of hydrodynamic phenomena like cavitation.

The Fig. 23 shows a comparison between a model without refinement on the left and a model that includes a refinement on the right.

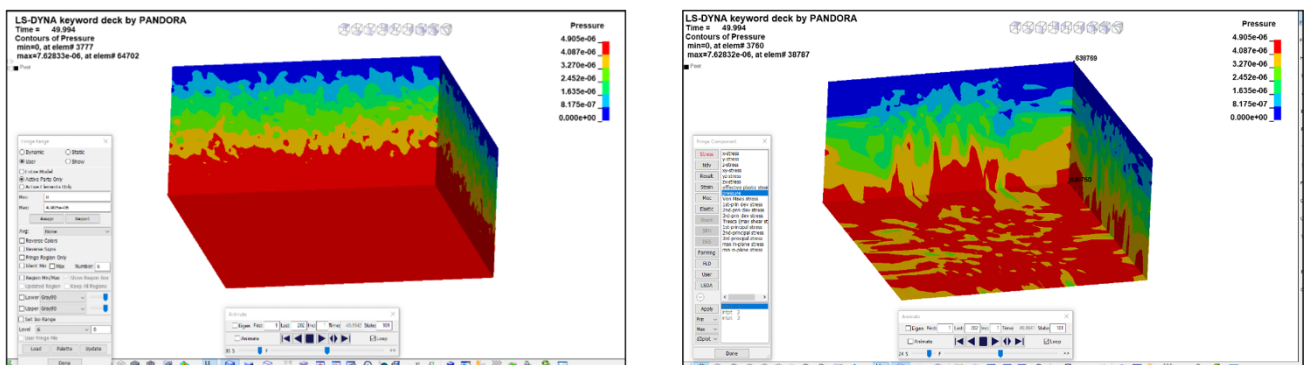


Figure 23: Comparison of the pressure distribution between models without (left) and with refinement (right)

One frame at 49.994 ms for both of simulations has been selected, the picture on the left shows a clear gradient of colors from blue on the top to red of the bottom with the increase of the pressure according to Stevin's law. Unlike in the picture on the right where the gradient is not as clear as the previous case and the pressure is not distributed homogeneously, this can be observed above all on the bottom of the basin.

4.3.3 Numerical results

The first parameter to compare to experimental results [4] is the reaction force perpendicular to the movement of the guided panel. In Fig. 24 the blue curve comes from the ALE model, instead the black curve is obtained from experimental reaction forces. For the first 28 ms the force is well represented by the ALE model, then the experimental curve continues to increase until the maximum value of 47.5 kN around 48 ms, instead the ALE curve has less growth. The ALE curve has his highest value at around 48 ms too, reaching the value of 31 kN, 16.5 kn and 34.7% less than the experimental curve. After 48 ms the distance between the two curves increases reaching an average of about 20 kn.

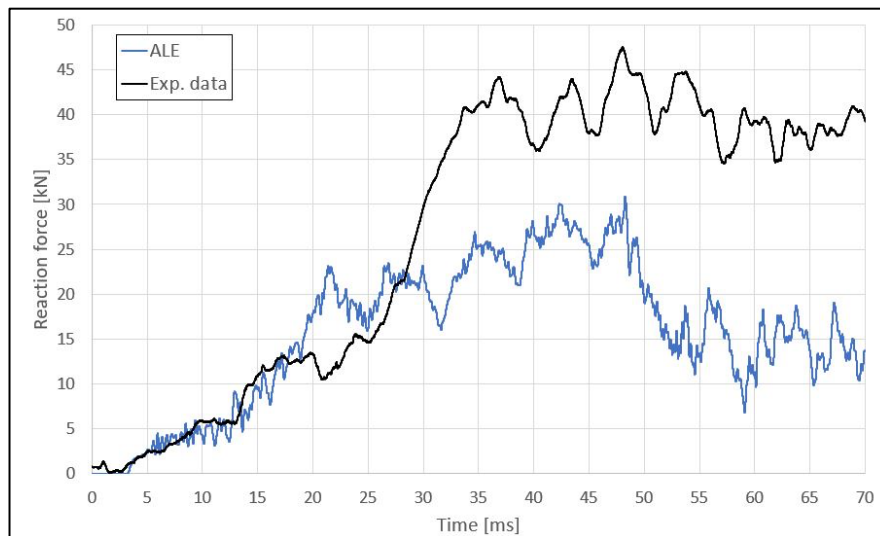


Figure 24: Comparison of the reaction force between ALE model and experimental data

ALE results from the probes on the front part of the panel are shown (Fig. 25). The shape of the curves is like the pressures obtained with the flat panel: an initial peak and then a decrease of the curve along the entire simulation; there is still the periodic return of the curves to zero and then again to the actual value, this behavior is more evident in the probes P24, P28 and P30.

In Fig. 26 the results of the rear sensors are shown and compared to the experimental data. The curves start from the reference ambient pressure of $1.01325E-04$ GPa and the cavitation occurs when the value goes below 2.7 kPa. According to the black curves, around 10 ms the cavitation should occur until 30 ms when ventilation occurs, and the pressure returns around to the ambient value. For ALE curves these two phenomena don't take place.

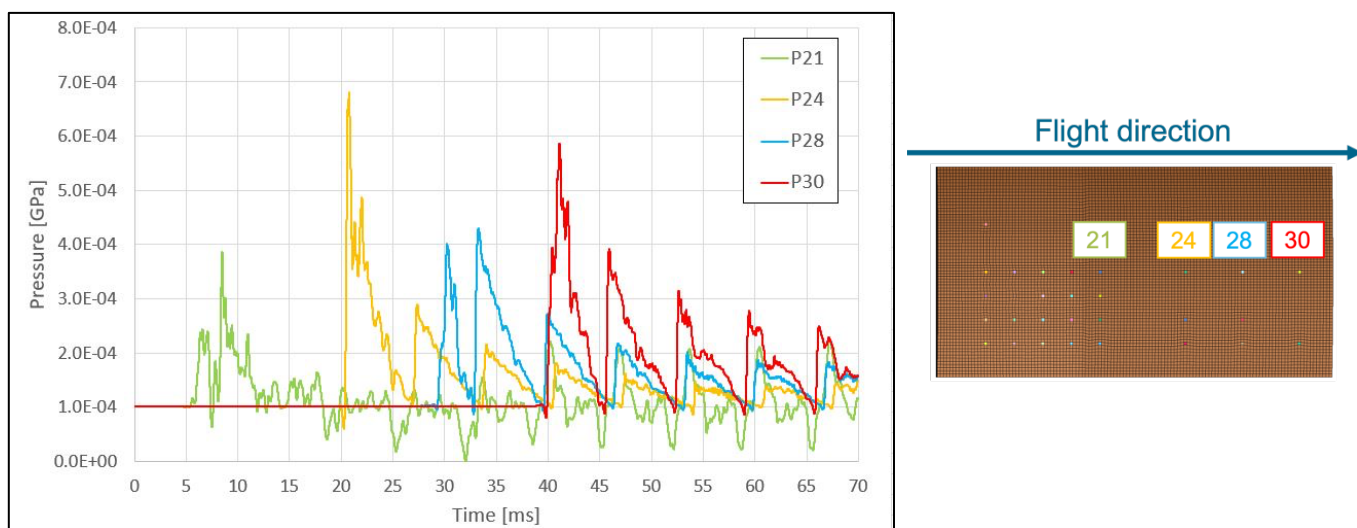


Figure 25: Pressure for the front probes of the DCP

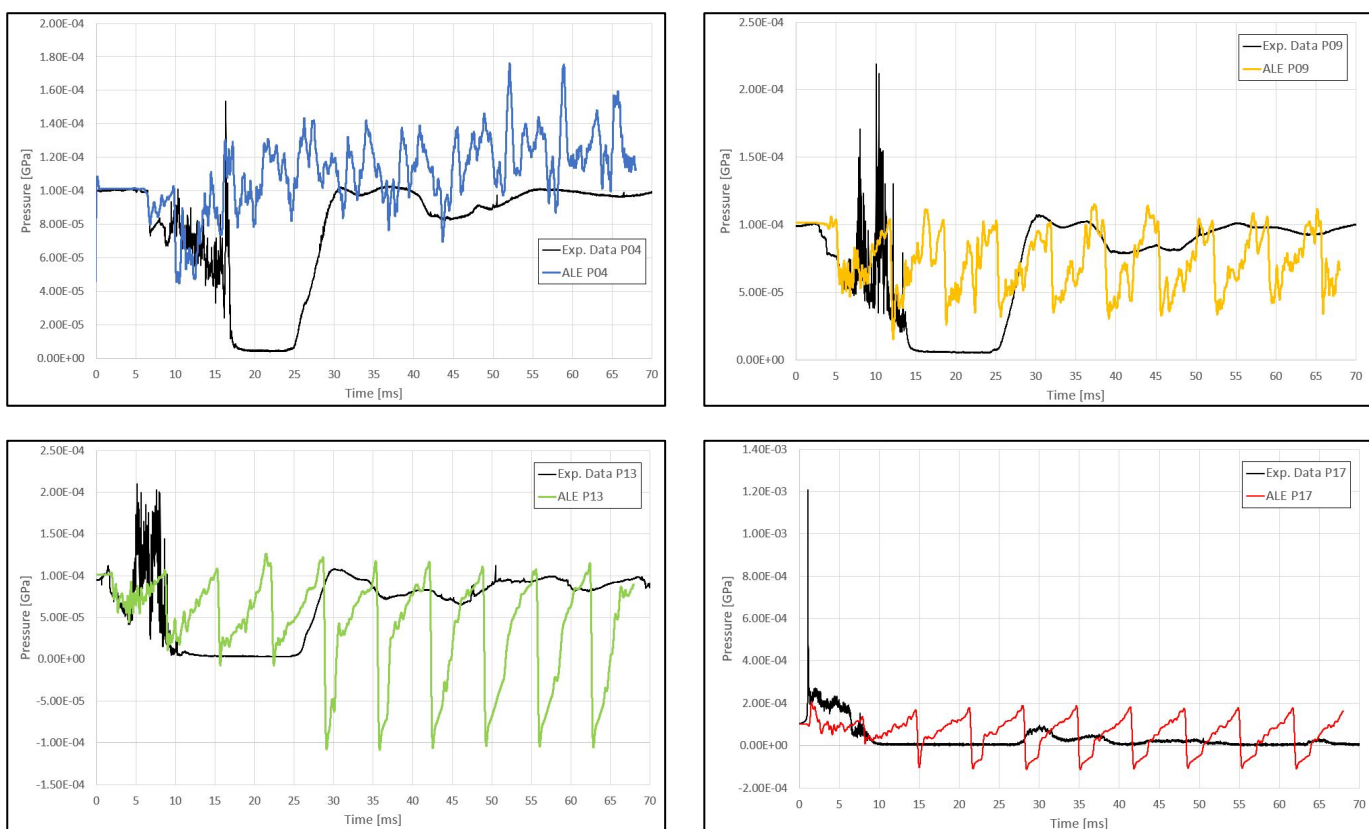


Figure 26: Comparison of the pressure between ALE model and experimental data [13] for the rear probes of the DCP

In the Fig. 27 the progress of the simulation is shown.

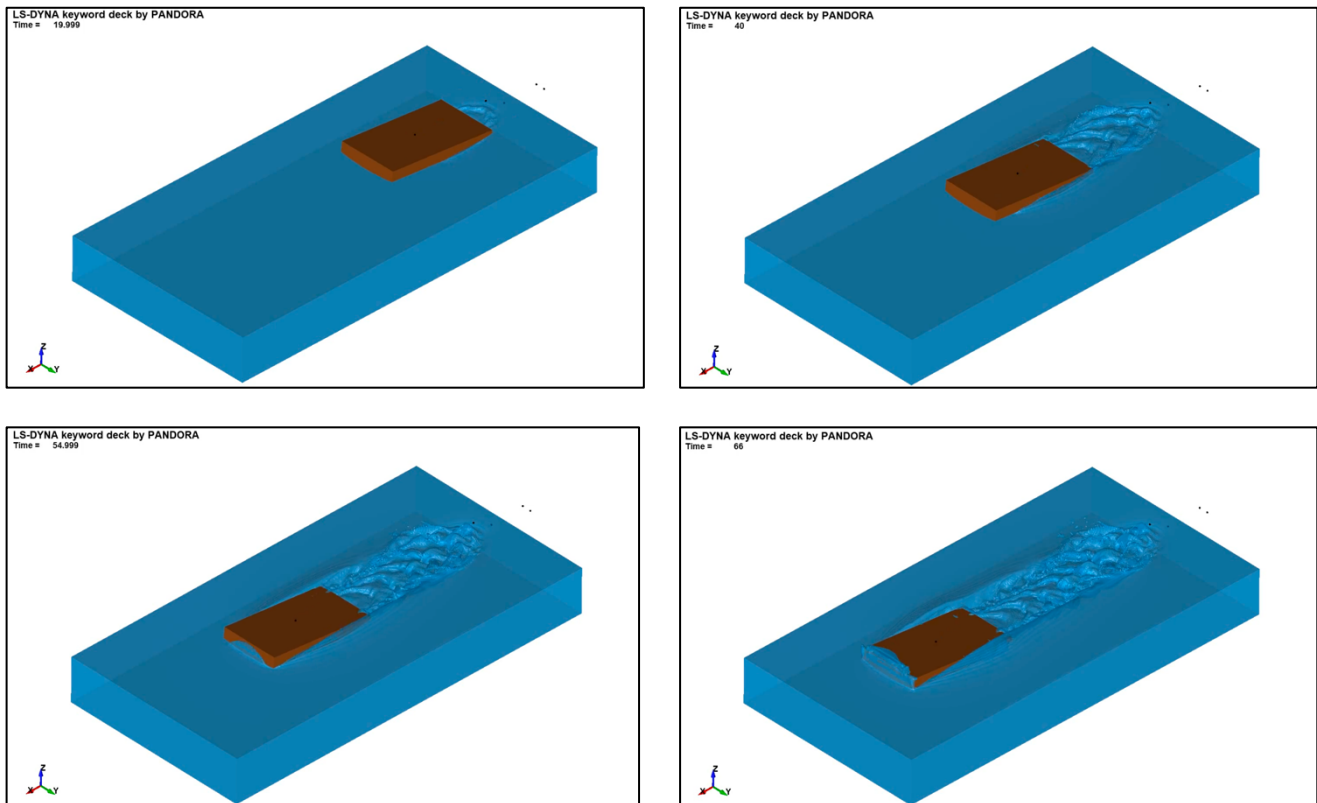


Figure 27: DCP simulation at 20 ms, 40 ms, 55 ms and 66 ms from top left to the right bottom

In the table 10 some computational outputs for DCP are shown.

Elapsed time	Iterations	Smallest TS	Nodes	Cores	Solver version
32h 43' 05''	55 012	1.27E-03 ms	3	24	R13.1

Table 10: Computational results for the Double-Curved Panel

4.3.4 Conclusion

This benchmark represents the real part of the fuselage that impacts first the water during ditching events and hydrodynamic phenomena are expected. The model had several adjustments compared to the previous benchmark: the refinement was deleted due to its influence on the hydrostatic pressure; vacuum was replaced by air setting the reference ambient pressure for both water and air; the parameters DIREC and EBC changed respectively their values from 2 and 0 to 1 and 1. Despite the reduction of the air domain height and the increase of cores, the simulation took almost 32 hours, 3 times the elapsed time of the flat panel. The air instead the vacuum influences on the increase of the elapsed time, but it is needed to set a reference pressure also for the upper basin.

To simulate properly the hydrodynamic phenomena the ALE model needs to be analyzed more in detail introducing new parameters not analyzed in this study.

4.4 D150 rigid aircraft

All the new features related to ALE method are now implemented in the D150. It is an aircraft generated at DLR, it is similar to a commercial fixed-wing single-aisle aircraft used for short-mid range missions, it can hold 150 passengers [19]. This model has been already analyzed in the research project ADAWI [20] in collaboration between DLR and ONERA. The Fig. 28 shows the dimension of the D150 model.

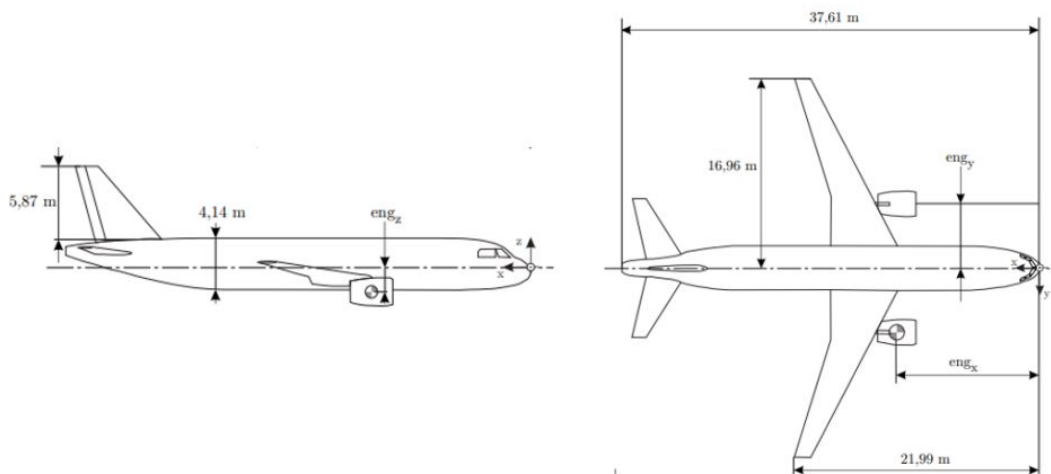


Figure 28: Dimension D150 Aircraft [6]

4.4.1 Numerical model

The model includes the D150 structural model and two basins, water and air (Fig. 29). Like the flat panel there is a refinement area in this model. The model has a forward velocity of 70 m/s and a sink rate of 1.5 m/s, a pitch angle of 8° and the total mass of the rigid body is 72547 kg.

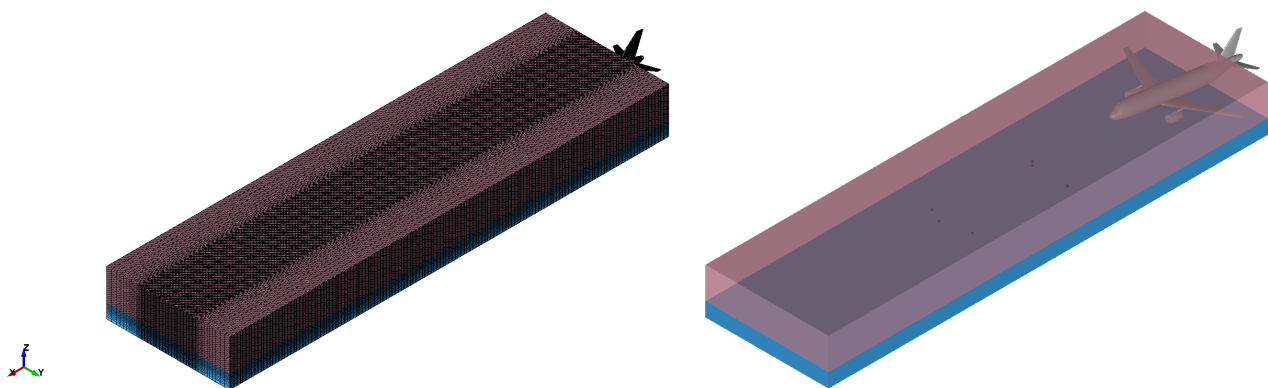


Figure 29: D150 model on LS-DYNA: a) water and air mesh; b) water, structural model and air.

To reduce computational time, the pool starts shortly before the impact leaving the rear part and the tail out of the basins. The height of the air has not been reduced in this model.

For this model DIREC = 1 and EBC = 1 and the properties of the water and air are the same of the DCP panel also setting the reference ambient pressure. The gravity is constant for all the simulation time of 500 ms, the lift is linear: starts at $t = 0$ ms equal to the gravitational acceleration times the total mass of the rigid body until the end of the simulation when its value is set to 0.

In the table 11 are shown info about moments of inertia.

lxx	lxy	lxz	lyy	lyz	lzz
1.137E+12	2.681E+06	-9.350E+10	3.221E+12	3.656E+05	4.276E+12

Table 11: Moments of inertia of D150. All the parameters are in $\text{kg}\cdot\text{mm}^2$

The tables 12 and 13 show general parameters about the water and air domains.

Size water domain (length x, width y, height z)	Size air domain (length x, width y, height z)	N. elements of water	N. elements of air
(88, 35, 4) m	(88, 35, 9) m	708 400	2 125 200

Table 12: Water and air basins setting

Mesh water refinement size	Length x direction	Width y direction	Height z direction
200 mm	88 m	15.8 m	1.5 m

Table 13: Refinement setting

4.4.2 Numerical results

Fig. 30 shows the pitch angle, after the impact at 70 ms the suction force applied to the fuselage causes the aircraft to pitch up reaching the maximum value around 390 ms of the pitch angle of 11.6° , after 500 ms it is equal to 10.7° .

Regarding the contact force, it has been obtained from the output file *dbfsi*, generated when the card ***Database_fsi** is set. It represents the force of the fluid-structure interaction. In Fig. 31 is shown that the contact force doesn't increase in value until 175 ms when the increase is net. The peak of the contact force is at 300 ms, it is equal to 2360 kN. Then there is a rapid decrease of the curve below to zero from 425 ms to the end of the simulation.

Looking at the displacement of the center of mass along z direction in the Fig. 32, it's possible to see a not physically possible bounce of the aircraft that starts at 325 ms until 450 ms, then the D150 model starts to descend again

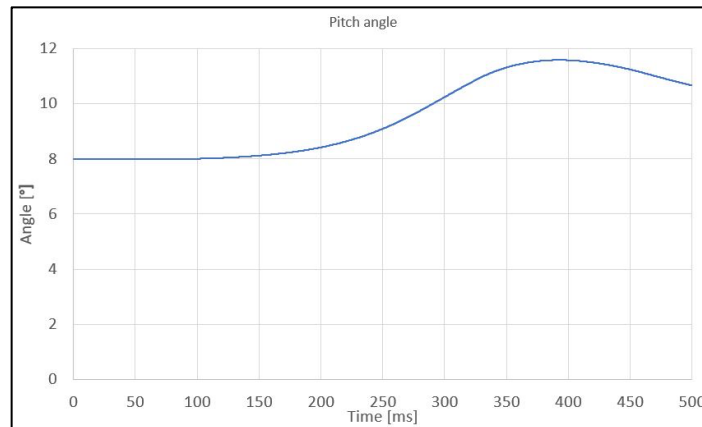


Figure 30: Pitch angle D150

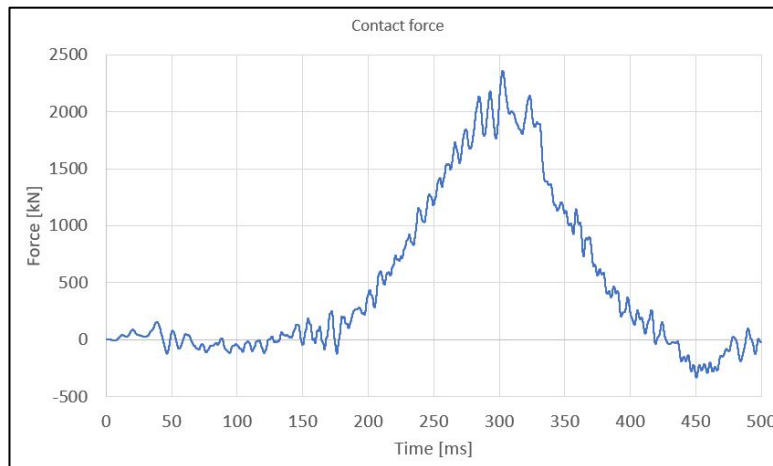


Figure 31: Contact force D150

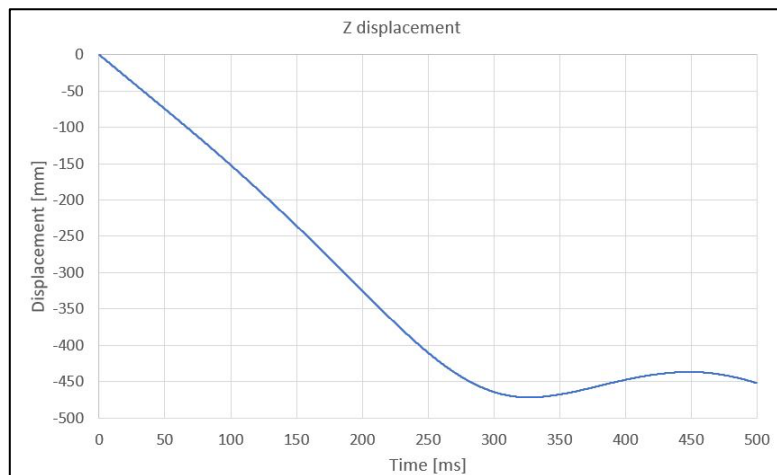


Figure 32: Displacement along Z direction of the D150 COG

In the Fig. 33, 4 moments of the D150 simulation are shown.

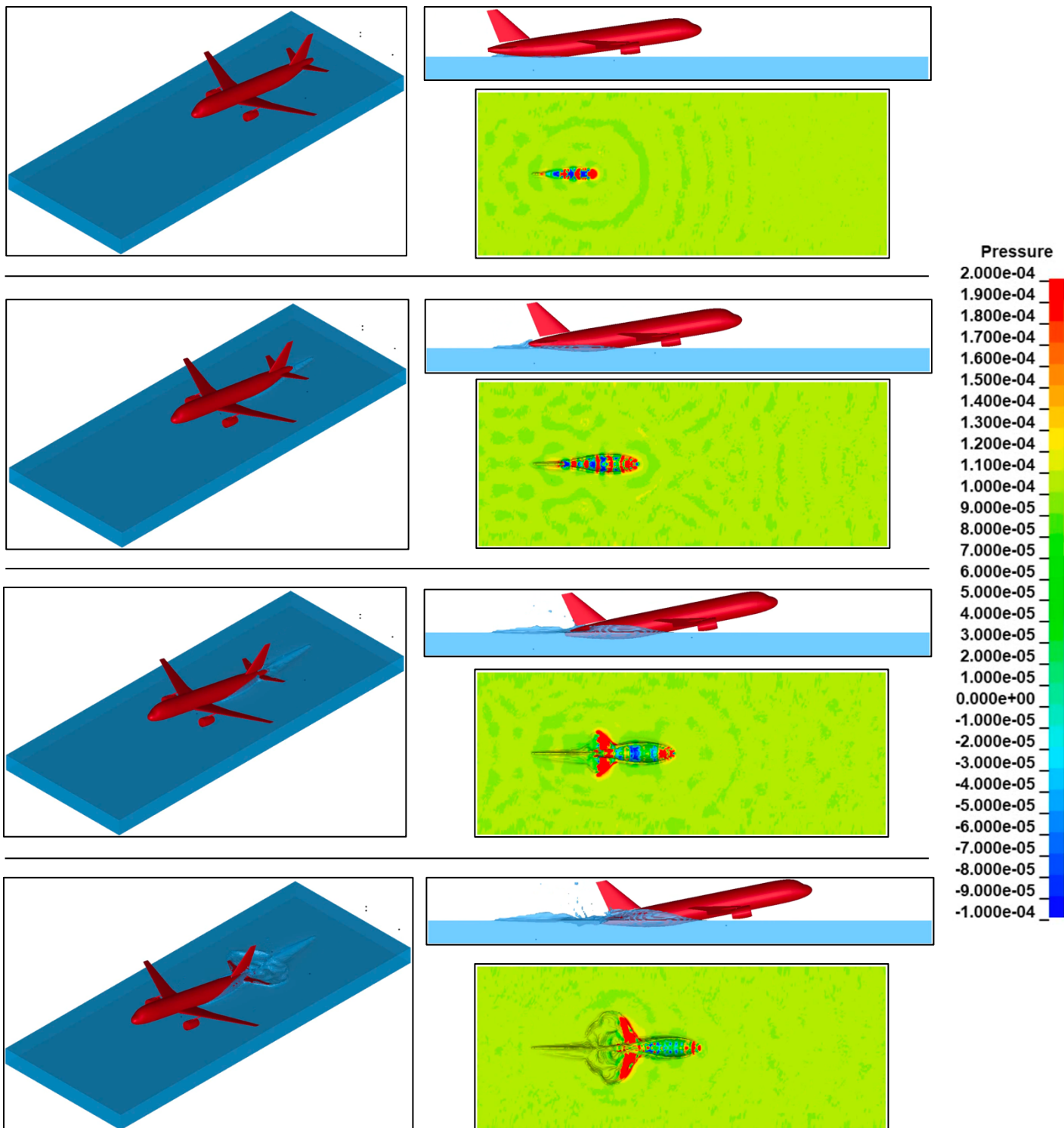


Figure 33: D150 simulation (iso and left side view) and pressure (top view) at 150 ms, 250 ms, 350 ms and 450 ms from top to the bottom

In the table 14 some computational outputs for D150 are shown.

Elapsed time	Iterations	Smallest TS	Nodes	Cores	Solver version
37h 00' 42''	65 558	7.63E-03 ms	3	24	R13.1

Table 14: Computational results for D150

4.4.3 Conclusion

Beyond the model that includes air presented in this report, other studies with void have been made, however the behavior of the water was not appropriate, for this reason it is not part of the study for D150. Then air replaced vacuum with the same properties and initial reference pressure of DCP.

Regarding the results, the suction effect is represented, after the impact the tail of the aircraft sinks causing the aircraft to pitch up until 11.6° . The simulation time of 500 ms is not enough to allow the impact of the engines too.

5 Conclusion and Outlook

5.1 Conclusion

This study has been started to analyze different models with the ALE method in LS-DYNA and compare the results with the experimental data or results from previous simulations using alternative modelling approaches or software packages. The project counts 4 models:

1. Rigid Sphere impacts water with a vertical movement.
2. Guided ditching of a single flat aircraft panel from the SMAES project.
3. Guided ditching of a double-curved aircraft panel from the SARAH project.
4. A ditching of a rigid single-aisle aircraft model from the ADAWI project.

After an initial period of familiarization with the method with the first model above mentioned, improvements have been made for each model, studying several parameters of new cards on LS-DYNA. In terms of kinematics a proper setup is now possible, setting the constrained path for guided motion models and the velocity in local coordinates for rigid body. The gravity is well set now with the card ***Load_body_z**. About pressure, it's important to know that the elements at the interface of the two basins must have the same size, moreover, the refinement has an influence on the distribution of the pressure on the water from the top to the bottom.

During this study, some tests to have the most appropriate setup have been performed, one of them regarded how to apply SPCs in the model, to avoid losing fluid decreasing its volume, all the outermost nodes of water and the upper basin must be fixed.

Focusing on the model results, the kinematic is well represented for both types of guided and non-guided models. The setup of the pressure needs to be studied more, results from flat panel are comparable to the experimental data even if underestimated. Moving on the next model where cavitation and then ventilation are expected, currently the rear sensors on ALE model cannot calculate properly the pressure reaching results comparable to experimental data.

In general, the ALE method is expensive in terms of computational time, including air instead of vacuum the elapsed time increases even more. To reduce computational time, there are three possible ways: to reduce the height of the upper basin; to set a refinement area considering its influence on the pressure; To put the rear part of the lagrangian structure of the basin considering the impact at the very begin of the pool and avoiding a long free flight period.

5.2 Outlook

In this study only rigid body have been analyzed, it's interesting to extend the ALE method investigation for flexible model studying the strain of the structure.

About pressure there are some cards and parameter that can improve the results, like ***Damping_part_mass** that should delete the continue oscillations between the reference value and

the effective value, or ***Initial_hydrostatic_ale** that improve the assessment of the pressure on the model. There is also the parameter *pref* representing a pseudo reference pressure equivalent to an environmental pressure that is being applied to the free surfaces of the ALE domain.

To improve ALE method to simulate hydrodynamic phenomena it needs to study more in detail considering the *Pressure Cutoff* parameter in the ***Mat_null** card.

To reduce computational time, an improvement to be added to next models is the possibility to include a refinement in z direction for the upper basin.

6 Bibliography

- [1] M. Siemann, "Numerical and Experimental investigation of the Structural Behaviour during Aircraft Emergency Landing on Water", 2016.
- [2] M. Siemann and B. Langrand, "Coupled fluid-structure computational methods for aircraft ditching simulations: Comparison of ALE-FE and SPH-FE approaches", *Computer & Structures*, 2017.
- [3] A. Iafrati and S. Grizzi, "Experimental Investigation of Fluid-Structure Interaction Phenomena During Aircraft Ditching", *AIAA Journal*, 2020.
- [4] A. Iafrati and S. Grizzi, "Cavitation and ventilation modalities during ditching", *Physics of Fluids*, 2019.
- [5] J. Donea, A. Huerta, J.-P. Ponthot e A. Rodríguez-Ferran, "Arbitrary Lagrangian-Eulerian Methods", *The Encyclopedia of Computational Mechanics*, vol. I, pp. 413-437, 2004.
- [6] DYNAmore Express, "Arbitrary-Lagrangian-Eulerian (ALE) method", 6th May 2022. [Online]. Available: <https://www.dynamore.de/en/downloads/presentations>.
- [7] Livermore Software Technology, "Theory manual", 2022.
- [8] L. Olovsson, M. Souli, I. Do, "LS-DYNA – ALE Capabilities (Arbitrary-Lagrangian-Eulerian) Fluid-Structure Interaction Modeling", Livermore Software Technology Corporation, 2003).
- [9] M. Petsch, D. Kohlgrüber and J. Heubischl, "PANDORA - A python based framework for modelling and structural sizing of transport aircraft", 2022.
- [10] T. Nouhaillaguet, "Implementation of a Python module for an automatic pool generation to be used in water impact simulation", 2022.
- [11] "SMAES Project Overview", 2014 [Online]. Available: <https://cordis.europa.eu/project/id/266172>
- [12] "SARAH Project Overview", 2020 [Online]. Available: <https://cordis.europa.eu/project/id/724139>
- [13] M. Pedelaborde-Augas, D. Kohlgrüber, C. L. Muñoz and M. Petsch, "Ditching simulation: Evaluation of different FSI-methods in LS-DYNA and VPS", 2021.
- [14] M. Anghileri and A. Spizzica, "Experimental Validation of Finite Element Models for Water Impacts", Second International Crash Users, Cranfield Impact Centre, England, 26-28 June 1995.
- [15] A. Topa, "Youtube", 12 October 2020. [Online]. Available: <https://www.youtube.com/watch?v=yq4jVpvkbb0&t=595s>.
- [16] N. Toso, "Contribution to the modelling and simulation of aircraft structures impacting on water", 2009.
- [17] Livermore Software Technology, "LS-DYNA keyword user's manual", vol. II, 2022.
- [18] Livermore Software Technology, "LS-DYNA keyword user's manual", vol. I, 2022.
- [19] C. Leon Muñoz, D. Kohlgrüber, M. Petsch and M. Pedelaborde-Augas, "Analysis of the application of fuselage skin reinforcements with beam element representations in flexible full aircraft models for ditching simulations", *IOP Conf. Ser.: Mater. Sci. Eng.*, 2022.
- [20] D. Kohlgrüber, L. Bertrand and M. Siemann, "DLR/ONERA Project ADAWI (Assessment of Aircraft Ditching and Water Impact); Recent progress to model full aircraft ditching", Rome, Italy, 04 October 2018.